TURBULENCE MEASUREMENTS FROM 5-BEAM ACOUSTIC DOPPLER CURRENT PROFILERS

Maricarmen Guerra Paris* and Jim Thomson

Applied Physics Laboratory, University of Washington, Seattle, Washington

**Corresponding author address:* Maricarmen Guerra Paris, Applied Physics Laboratory, University of Washington, 1013 NE 40th Street, Box 355640, Seattle, WA 98105-6698.

E-mail: mguerrap@uw.edu

ABSTRACT

Two new 5-beam Acoustic Doppler Current Profilers, the Nortek Signature 1000 AD2CP and the Teledyne RDI Sentinel V50, are demonstrated to measure turbulence at two energetic tidal channels within Puget Sound, WA, USA. The quality of the raw data is tested by analyzing the turbulent kinetic frequency energy spectra, the turbulence spatial structure function, the shear in the profiles, and the covariance Reynolds stresses. The Nortek's low Doppler noise and high sampling frequency allow for the observation of the turbulent inertial subrange in both the frequency spectra and in the structure function. The five-beam configuration allows for a direct estimation of the Reynolds stresses from along-beam velocity fluctuations. These combined results are then used to assess a turbulent kinetic energy budget, in which depth profiles of the turbulent kinetic energy dissipation and production rates are compared. The associated codes are publicly available at the Matlab File Exchange website.

1. Introduction

Acoustic Doppler Current Profilers (ADCPs) are commonly used to measure the three components of fluid velocities along depth profiles in the ocean using three or four diverging acoustic beams. The raw measurements are typically burst-averaged in time in order to reduce the Doppler noise inherent to the method, which can add significant variance to the raw signals (above and beyond the variance due to real turbulent fluctuations) (Brumley et al. 1991). However, if the raw data of along-beam velocities are retained, many turbulence parameters, such as Reynolds stresses and turbulent kinetic energy dissipation rates, can be estimated from ADCP measurements. Estimation methods are based on the variance and correlations of the along-beam velocity fluctuations, often with explicit removal of the variance contributed by the Doppler noise (Lu and Lueck 1999; Stacey et al. 1999; Wiles et al. 2006; Thomson et al. 2012).

In the frequency domain, some authors have attempted to use spectra calculated from raw ADCP data, but the inherent Doppler noise typically obscures the expected turbulent cascade of eddies to higher and higher frequencies through the inertial subrange (Richard et al. 2013). Recently, turbulence dissipation rates were estimated from turbulence spectra after averaging the frequency spectra for different mean flows and bins in order to observe the isotropic turbulence energy cascade in McMillan et al. (2016). Another common technique is to estimate turbulent dissipation rates using the second-order spatial structure function of turbulence, which is based on Kolmogorov's theory of a turbulent cascade of eddies at smaller and smaller length scales (Wiles et al. 2006; Rusello and Cowen 2011).

One of the most frequently used techniques to estimate Reynolds stresses is the variance technique (Lu and Lueck 1999; Stacey et al. 1999; Rippeth et al. 2003), which provides two components (out of six) of the Reynolds stresses and is based in the variance of opposite beam velocity fluctuations.

A new generation of broadband ADCPs with the ability to measure flow velocity at higher frequencies and with lower noise levels is poised to expand routine turbulence measurements. Moreover, the inclusion of a fifth beam allows for a true measurement of vertical velocities and the estimation of five (out of six) Reynolds stresses, total turbulent kinetic energy (TKE), and anisotropy directly from the along-beam velocities (Lu and Lueck 1999; Dewey and Stringer 2007). This is a notable expansion beyond the four-beam variance methods (Lu and Lueck 1999; Stacey et al. 1999; Rippeth et al. 2003).

In this paper we present turbulence measurements from a new five-beam Nortek Signature 1000 (kHz), which uses the acronym AD2CP to distinguish it from the previous generation of profilers, and also from a new Teledyne RDI Sentinel V50 500 (kHz). The new instruments' capabilities are assessed in two field deployments in tidal channels, calculations of turbulence parameters, and the subsequent evaluation of turbulent kinetic energy (TKE) budgets.

2. Data Collection

a. Site Description

Turbulence measurements were taken at Admiralty Inlet (AI) and Rich Passage (RP), two tidal channels located in Puget Sound, WA, USA. The map of Figure 1a shows the location of AI and RP within Puget Sound and the detailed locations of the instruments.

Admiralty Inlet is located in the northern part of Puget Sound (48.14°N, 122.71° W). AI is ~ 6.5 km wide and ~ 50 m deep at the measurement site. The principal direction of the flow is $\sim 50°$ from the east in the clockwise direction.

Rich Passage is located south of Bainbridge island in Puget Sound (47.59° N, 122.56° W). At the measurements site the channel is ~ 28 m deep and ~ 550 m wide. The channel is oriented $\sim 45°$ from north in the clockwise direction.

b. Instruments and Settings

The 5-beam Doppler profilers were deployed mounted looking upward on separate Oceanscience Sea Spider tripods, which place each instrument ~ 0.9 m above the seafloor when deployed. The instruments have four beams slanted at 25°, plus a fifth vertical beam. Deployments were on 11 May 2015 at AI and on 17 – 18 May 2015 at RP.

The Nortek Signature was configured to measure turbulence in along-beam coordinates using its 5 beams at 8 Hz (the maximum possible when using all five beams) for 10 minute bursts. At AI, the burst interval was 20 minutes and there were 20 velocity bins at 1 m spacing. At RP, the burst interval was 30 minutes and there were 15 velocity bins at 1 m spacing.

The Teledyne RDI Sentinel V50 was configured to measure along-beam turbulent velocities at 2 Hz (the maximum possible when using all five beams) for 10 minute bursts with a 20 minute interval. At AI, the Sentinel V50 tripod was ~ 50 m away from the Signature tripod and there were 20 velocity bins at 1 m spacing. At RP, the Sentinel V50 was not deployed (it was unavailable).

c. Raw Data

Figure 2 shows the vertical profiles and a time series of along channel velocity (after a coordinate transformation of the beam velocities) measured by the Nortek Signature for both study sites. At AI, it was possible to measure only a single tidal cycle due to the rapid battery consumption when sampling at high frequency. At RP, a reduced duty cycle made it possible to measure two tidal cycles. Although these are short datasets, they are sufficient to observe turbulent velocity fluctuations at a wide range of mean flows at each site (e.g., burst-averaged varied from 0 to 2 m/s). Data are quality controlled to remove measurements with low beam correlations and low echo amplitude (less than 0.5% of the raw data).

3. Analysis: Turbulent Kinetic Energy Dissipation Rate

At each depth in the measured profile, the TKE dissipation rate is estimated by two methodologies: from the frequency spectra (Lumley and Terray 1983) and from the spatial structure function (Wiles et al. 2006). Both methods require the observation of the inertial subrange of isotropic turbulence.

a. Turbulent Kinetic Energy Spectra

Vertical beam velocities are used to estimate the vertical turbulent kinetic energy frequency spectra. TKE spectra are estimated using Welch's Overlapped Segment Averaging method. For the Nortek Signature data sets, spectral estimates are calculated for every ten-minute burst using 23 50 s sub-windows with 50% overlap and a Hanning data taper, which results in an ensemble spectral density estimate with ~ 45 degrees of freedom. TKE spectra with the same degrees of freedom are also estimated for the RDI Sentinel V50 vertical beam velocities.

TKE spectra estimates for both sites for the tenth vertical bin (10.4 m from the sea bottom) are presented in Figure 3. The TKE spectra estimates from the RDI Sentinel V measurements for the same bin are included in the AI figures in grey. All spectral density estimates are well sorted by mean flow velocity, except during the stronger ebb at RP, where the instrument is in the lee of a sill.

The most novel result from the Nortek Signature data is the clear observation of the TKE energy cascade in the spectral estimates, which is usually obscured by the Doppler noise of profiling instruments. An isotropic region of tridimensional turbulence is present at mid frequencies ($0.1 < f < 1$ Hz) which follows the classic $f^{-5/3}$ energy cascade (Kolmogorov 1941). At higher ($f > 1$ Hz) frequencies, the spectrum becomes affected by the instrument inherent Doppler noise. The spectral noise level of the Nortek Signature is observed around $S_w(f) = 10^{-4}$ m^{2}s^{-2}Hz^{-1}. The noise level of the RDI Sentinel V50, by contrast, is much higher at $S_w(f) = 10^{-2}$ m^{2}s^{-2}Hz^{-1}, and thus inertial subrange is obscured in those spectra. The higher noise level prevents the use of the RDI Sentinel V50 data in the analyses to follow.

The dissipation rate of TKE, ε, is related to the isotropic portion of the vertical TKE frequency spectrum by:

$$S_w(f) = \alpha \varepsilon^{2/3} f^{-5/3} \left(\frac{\bar{u}}{2\pi}\right)^{2/3} \tag{1}$$

where α is a constant equal to 0.69, ε is the TKE dissipation rate, f is the frequency and $\bar{u}$ is the mean along channel velocity. This applies Taylor's 'frozen field' hypothesis, in which the turbulence does not evolve as it advects past the instrument, such that we can transform the temporal observation into a spatial one (i.e., $f = 2\pi\bar{u}/k$), where k is the spatial wavenumber.

Each estimated spectra is multiplied by $f^{5/3}$ to get a compensated spectra in the inertial subrange. The dissipation rate is estimated by solving $\overline{S_w(f) f^{5/3}\Big|_{f_1}^{f_2}} = \alpha \varepsilon^{2/3} \left(\frac{\bar{u}}{2\pi}\right)^{2/3}$, where f_1 to f_2 is the frequency range with the slope closest to zero in the compensated spectra. A minimum of five frequencies are used to estimate dissipation rates from the compensated spectra.

b. Turbulence Structure Function

The along-beam velocities are used to estimate the second-order spatial structure function of the along-beam turbulent fluctuations $D(z,r)$ following the methodology described in Wiles et al. (2006). The structure function is defined as:

$$D_i(z,r) = \langle \left(u_i'(z+r) - u_i'(z)\right)^2 \rangle \tag{2}$$

where z is the along-beam measurement location, u_i' corresponds to each along-beam velocity fluctuation, and r is the distance between two velocity measurements; the angle brackets denote a time average over the burst.

The structure function $D_i(z,r)$ is estimated from the bottom of the profile upwards. The distance r is set to be positive and limited by the distance to the closest boundary, which in these cases is the sea bottom. Figure 4 shows examples of the spatial structure function for the vertical beam turbulent fluctuations, $D_5(z,r)$, at $z = 10.4$ m from the sea bottom at both sites. All structure functions are well-sorted by the mean flow, except during the stronger ebb at RP, where again the sill creates a region of low turbulence. The slope of the structure functions agrees well with the expected $r^{2/3}$ at both sites.

In the inertial subrange, the structure function is related to the distance r and to the dissipation rate ε by:

$$D_i(z,r) = C_v^2 \varepsilon^{2/3} r^{2/3} \tag{3}$$

where C_v^2 is a constant equal to 2.1 (Wiles et al. 2006; Thomson et al. 2012).

The structure function is multiplied by $r^{-2/3}$ to obtain a compensated structure function in the inertial subrange (Rusello and Cowen 2011). The dissipation rate is estimated by solving $\overline{D(z,r)r^{-2/3}\big|_{r_1}^{r_2}} = C_v^2 \varepsilon^{2/3}$, where r_1 to r_2 is the range with the slope closest to zero. Estimates are not calculated for depths with less than 4 points in the structure function. Within the valid depths, the structure function is quality controlled to remove estimates with negative slope, resulting in a 21% loss at AI and 28% loss at RP.

Figure 6 shows mean vertical profiles of TKE dissipation rates for both sites and compares the methods. The dissipation rate estimates from both methods are in agreement, although the estimates from the structure function do not cover the entire measured profile due to the r limitation.

4. Analysis: Turbulent Kinetic Energy Production Rate

In a well-mixed environment the production from buoyancy can be neglected and the TKE is primarily produced by the mean flow shear. If horizontal shear is small, the TKE production can be approximated in terms of the Reynolds stresses and the velocity vertical gradients as:

$$P = -\overline{u'_{ch}w'}\frac{\delta\overline{u_{ch}}}{\delta z} - \overline{v'_{ch}w'}\frac{\delta\overline{v_{ch}}}{\delta z} - \overline{w'w'}\frac{\delta\overline{w}}{\delta z} \tag{4}$$

where P is the production of TKE, u_{ch}, v_{ch} and w are the along channel, across channel and vertical velocities respectively, and the primes denote velocity fluctuations.

a. Vertical Shear

Along-beam velocities are transformed into orthogonal east-north-up components. The horizontal components are rotated to obtain along and across channel velocity components at each location. The vertical gradients of the along channel, across channel and vertical velocity, $\frac{\delta\overline{u_{ch}}}{\delta z}$, $\frac{\delta\overline{v_{ch}}}{\delta z}$, $\frac{\delta\overline{w}}{\delta z}$, are estimated as the centered difference of their burst-average using the vertical distance between measurements.

b. Reynolds Stresses

The Reynolds stress tensor is estimated following the methodology of Dewey and Stringer (2007) for a 5-beam ADCP configuration. This methodology extends the variance technique (Lu and Lueck 1999; Stacey et al. 1999; Rippeth et al. 2003) to different ADCP beam configurations including expressions for the Reynolds stresses for non-zero tilt. This method assumes small angle approximations for pitch and roll, which was achieved in these deployments (mean pitch $\sim 2.3^\circ$ and mean roll $\sim 0.4^\circ$ at AI, mean pitch $\sim 0.35^\circ$ and mean roll $\sim -1.19^\circ$ at RP). The Reynolds stresses from Dewey and Stringer (2007) are written in instrument coordinates (assuming heading is equal to zero), thus the obtained stresses are rotated to along and across channel coordinates after the calculations.

The following equations, from Dewey and Stringer (2007), define the Reynolds stresses in instruments coordinates for any 5-beam ADCP:

$$\begin{aligned}\overline{u'^2} = \frac{-1}{4\sin^6\theta\cos^2\theta}\{&-2\sin^4\theta\cos^2\theta(\overline{u_2'^2}+\overline{u_1'^2}-2\cos^2\theta\overline{u_5'^2}) \\ &+2\sin^5\theta\cos\theta\phi_3(\overline{u_2'^2}-\overline{u_1'^2})\}\end{aligned} \tag{5}$$

$$\begin{aligned}\overline{v'^2} = \frac{-1}{4\sin^6\theta\cos^2\theta}\{&-2\sin^4\theta\cos^2\theta(\overline{u_4'^2}+\overline{u_1'^3}-2\cos^2\theta\overline{u_5'^2})-2\sin^4\theta\cos^2\theta\phi_3(\overline{u_2'^2}-\overline{u_1'^2}) \\ &+2\sin^3\theta\cos^3\theta\phi_3(\overline{u_2'^2}-\overline{u_1'^2})-2\sin^5\theta\cos\theta\phi_2(\overline{u_4'^2}-\overline{u_3'^2})\}\end{aligned} \tag{6}$$

$$\begin{aligned}\overline{w'^2} = \frac{-1}{4\sin^6\theta\cos^2\theta}\{&-2\sin^5\theta\cos\theta\phi_3(\overline{u_2'^2}-\overline{u_1'^2}+2\sin^5\theta\cos\theta\phi_2(\overline{u_4'^2}-\overline{u_3'^2}) \\ &-4\sin^6\theta\cos^2\theta\overline{u_5'^2})\}\end{aligned} \tag{7}$$

$$\begin{aligned}\overline{u'w'} = \frac{-1}{4\sin^6\theta\cos^2\theta}\{&\sin^5\theta\cos\theta(\overline{u_2'^2}-\overline{u_1'^2})+2\sin^4\theta\cos^2\theta\phi_2(\overline{u_2'^2}+\overline{u_1'^2}) \\ &-4\sin^4\theta\cos^2\theta\phi_3\overline{u_5'^2}-4\sin^6\theta\cos^2\theta\phi_2\overline{u'v'}\}\end{aligned} \tag{8}$$

$$\begin{aligned}\overline{v'w'} = \frac{-1}{4\sin^6\theta\cos^2\theta}\{&\sin^5\theta\cos\theta(\overline{u_4'^2}-\overline{u_3'^2})-2\sin^4\theta\cos^2\theta\phi_2(\overline{u_4'^2}+\overline{u_3'^2}) \\ &+4\sin^4\theta\cos^2\theta\phi_3\overline{u_5'^2}+4\sin^6\theta\cos^2\theta\phi_3\overline{u'v'}\}\end{aligned} \tag{9}$$

where θ is the beam inclination angle (25° in these cases), ϕ_2 and ϕ_3 correspond to Dewey's pitch and roll respectively, and $\overline{u_i'^2}$ are the along-beam velocity fluctuation variances. For the Nortek Signature configuration: ϕ_2 corresponds to negative roll, and ϕ_3 to pitch, and $u_1 = u_{1Sig}$,

$u_2 = u_{3Sig}$, $u_3 = u_{4Sig}$, and $u_4 = u_{2Sig}$. For the RDI Sentinel V50 (not applied here): ϕ_2 corresponds to roll, and ϕ_3 to pitch, and $u_1 = u_{2Sent}$, $u_2 = u_{1Sent}$, $u_3 = u_{4Sent}$, and $u_4 = u_{3Sent}$.

The full Reynolds stress tensor is quality controlled to be a positive definite matrix, which results in a 12% loss of the Reynolds stresses at AI and in an 8% loss at RP.

Figure 5 shows vertical profiles of the estimated vertical shear Reynolds stress ($\overline{u'_{ch}w'}$), bin-averaged by mean flow. Again, Reynolds stresses are well-sorted by the mean flow, except during the stronger ebb at RP where the instrument is in the lee of a sill.

The estimated Reynolds stresses together with the vertical shear are used to estimate the vertical shear TKE production rate. Figure 6 shows averaged vertical profiles of TKE production for both sites separated by ebb and flood tides.

5. Application: Turbulent Kinetic Energy Balance

Assuming that the buoyancy term is negligible in these well-mixed sites and that self-advection is small, the rate of change of TKE can be approximated as

$$\frac{D}{Dt}(TKE) \approx P - \varepsilon \tag{10}$$

Figure 6 shows this balance as depth profiles of vertical shear production and TKE dissipation rates, which are averaged over all mean current speeds, for ebb and flood at each site. The expected balance is generally found, however there are distinct patterns that likely are related to the lateral headland at AI and the vertical sill at RP.

During ebb at AI, TKE production exceeds dissipation closer to the bottom and then dissipation exceeds production along most of the water column. During flood, dissipation is very close to production near the bottom and production exceeds dissipation in the higher portion of the water column. At RP, production exceeds dissipation in most cases.

6. Conclusions

A new 5-beam acoustic current profiler, the Nortek Signature 1000 (KHz) AD2CP, is successfully used to measure turbulence at two energetic tidal channels. TKE production and dissipation rates are estimated from the measurements, and an approximate TKE budget is obtained.

The results illustrate the capabilities of 5-beam profilers for assessing high order turbulence parameters. The frequency spectra from the Nortek Signature presents a low noise level, about $O(10^{-4})$ m^{2}s^{-2}, while the RDI Sentinel V50 presents a higher noise level of $O(10^{-2})$ m^{2}s^{-2} that is more similar to the previous generation of profilers. The lower noise level of the Nortek Signature enables observation of the inertial subrange of turbulence and thus improved estimations of the TKE dissipation rate. The use of all five beams enables the direct estimation the full Reynolds stress tensor and thus improved estimations of the TKE production rate.

The methods presented in this paper are implemented in Matlab and are available through the Matlab File Exchange website as 5-Beam Acoustic Doppler Current Profiler Turbulence Methods.

Acknowledgments. We thank Joe Talbert and Alex de Klerk for deployment and recovery of the instruments, and Andy Reay-Ellers for ship operations. Funding was provided by NAVFAC. Maricarmen Guerra thanks the Fulbright and the Conicyt Becas Chile doctorate fellowship programs.

References

Brumley, B. H., R. G. Cabrera, K. L. Deines, and E. A. Terray, 1991: Performance of a broad-band acoustics Doppler current profiler. *J. Ocean. Eng.*, **16 (4)**.

Dewey, R., and S. Stringer, 2007: Reynolds stresses and turbulent kinetic energy estimates from various adcp beam configurations: Theory. *J. Phys. Oceanogr.*, 1–35.

Kolmogorov, A., 1941: Dissipation of energy in the locally isotropic turbulence. *Dokl. Akad. Nauk SSR*, **30**, 301–305.

Lu, Y., and R. Lueck, 1999: Using a broadband adcp in a tidal channel. part ii: Turbulence. *J. Atmos. Oceanic Technol*, **16 (11)**, 1568–1579.

Lumley, J. L., and E. A. Terray, 1983: Kinematics of turbulence convected by a random wave field. *J. Phys. Oceanogr.*, **13**, 2000–2007.

McMillan, J., A. Hay, R. Lueck, and F. Wolk, 2016: Rates of dissipation of turbulent kinetic energy in a high reynolds number tidal channel. *J. Atmos. Oceanic Technol*, **33 (4)**, 817–837.

Richard, J., J. Thomson, B. Polagye, and J. Bard, 2013: Method for identification of doppler noise levels in turbulent flow measurements dedicated to tidal energy. *Int. J. Marine Energy*, **3**, 52–64.

Rippeth, T., J. Simpson, E. Williams, and M. Inall, 2003: Measurement of the rates of production and dissipation of turbulent kinetic energy in an energetic tidal flow: Red wharf bay revisited. *J. Phys. Oceanogr.*, **33 (9)**, 1889–1901.

Rusello, P., and E. Cowen, 2011: Turbulent dissipation estimates from pulse coherent doppler instruments. *Proc. IEEE/OES 10th Current, Waves and Turbulence Measurements (CWTM), Monterey, CA.*, IEEE, 167–172.

Stacey, M., S. Monismith, and J. Burau, 1999: Measurements of reynolds stress profiles in unstratified tidal flow. *J. Geophys. Res.*, **104**, 10 935–10 949.

Sutherland, D., P. MacCready, N. Banas, and L. Smedstad, 2011: A Model Study of the Salish Sea Estuarine Circulation. *J. of Phys. Oceanogr.*, **41 (6)**, 1125–1143.

Thomson, J., B. Polagye, V. Durgesh, and M. Richmond, 2012: Measurements of turbulence at two tidal energy sites in Puget Sound, WA. *IEEE J. Oceanic Eng.*, **37 (3)**, 363–374.

Wiles, P. J., T. P. Rippeth, J. H. Simpson, and P. J. Hendricks, 2006: A novel technique for measuring the rate of turbulent dissipation in the marine environment. *Geophys. Res. Lett.*, **33 (21)**.

LIST OF FIGURES

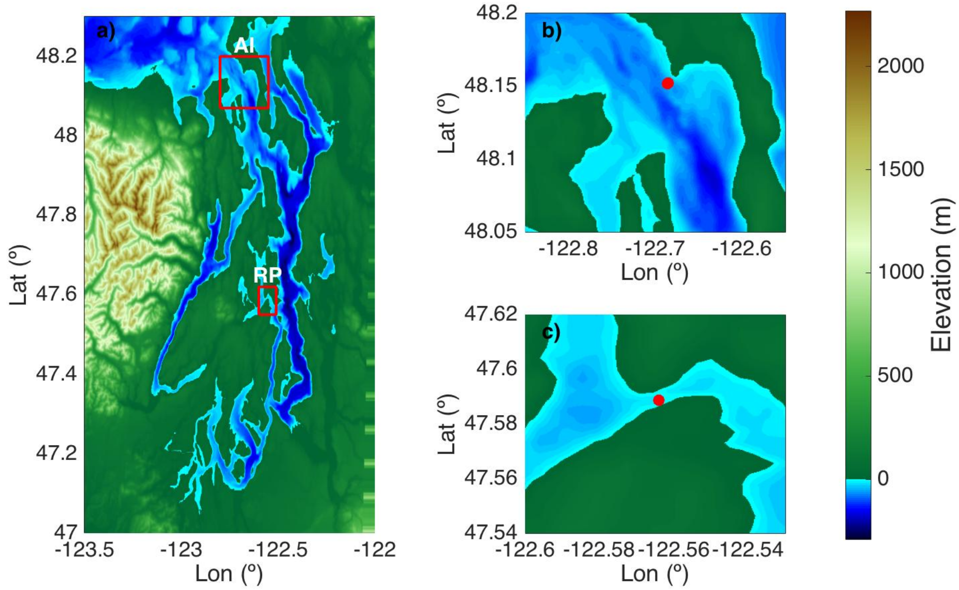

FIG. 1. Bathymetry and location of instruments: a) Puget Sound in Washington, U.S.A., b) Admiralty Inlet (AI) and c) Rich Passage (RP). Red dots indicate instruments location.

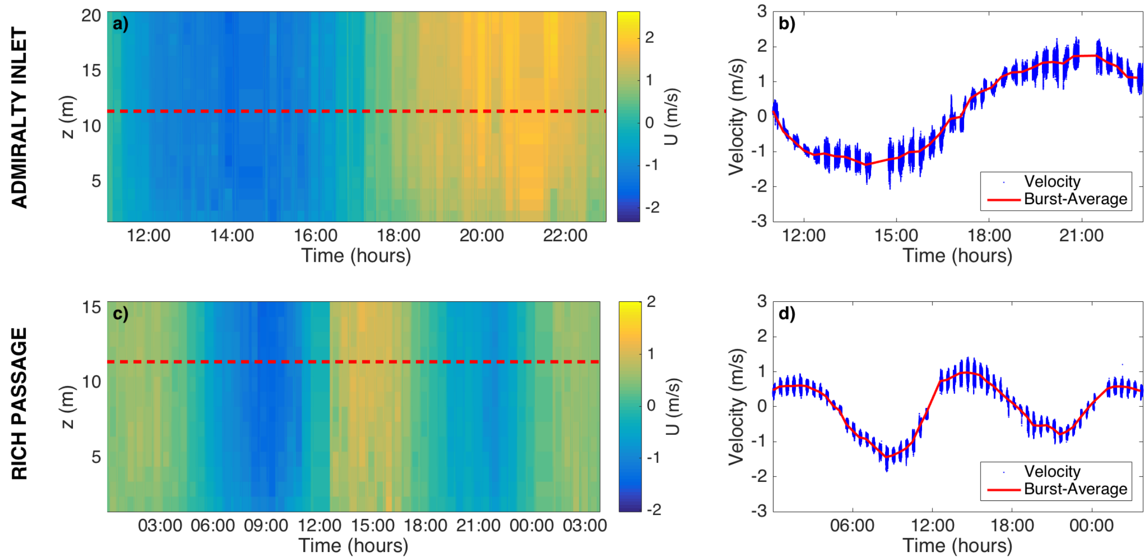

FIG. 2. Vertical profiles and time series of along-channel velocities: a), b) from AI, and c), d) from RP. Red dashed line indicates depth corresponding to the time series (as $z = 10.4$ m from sea-bottom).

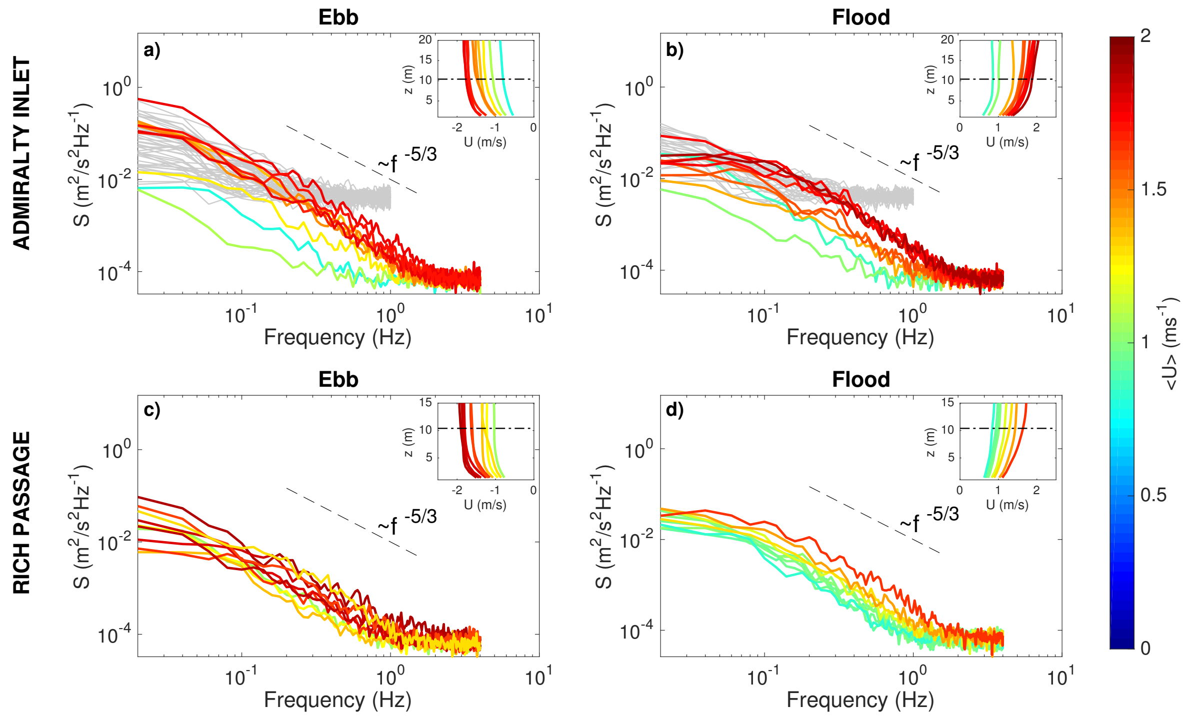

FIG. 3. TKE spectra at $z = 10.4$ m for different mean flows (by color): a), b) at AI, and c), d) at RP. Dashed line is proportional to $f^{-5/3}$. Inset plots show mean flow vertical profiles (also by color); dot-dashed line shows $z = 10.4$ m in the profiles. In the AI plots, spectra from the RDI Sentinel V50 data are included as grey curves.

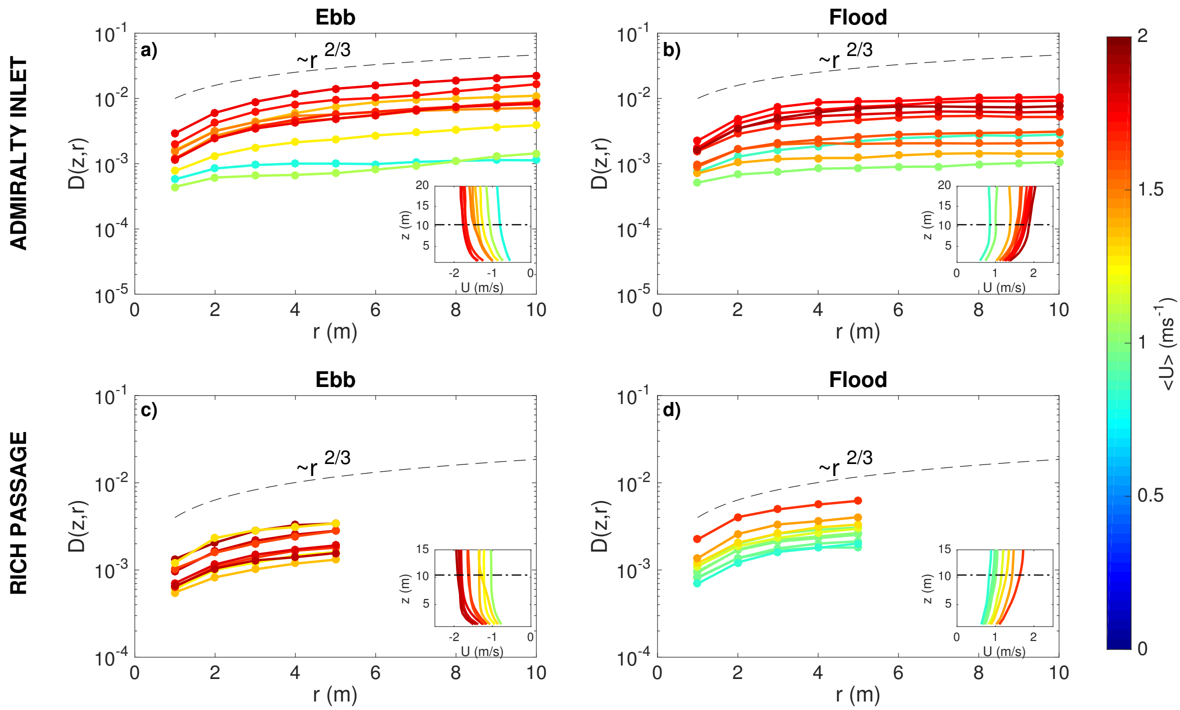

FIG. 4. Spatial structure function at $z = 10.4$ m for different mean flows (by color): a), b) at AI, and c), d) at RP. The dashed line is proportional to $r^{2/3}$. Inset plots show mean flow vertical profiles (also by color); the dot-dashed line corresponds to $z = 10.4$ m.

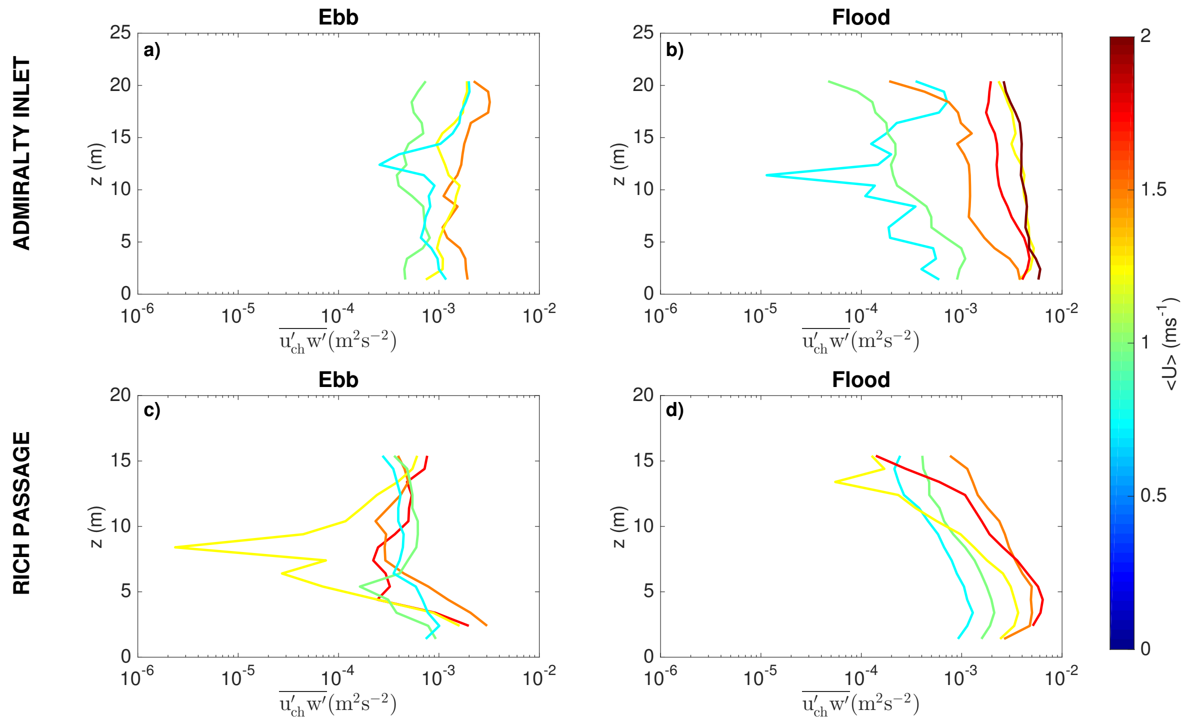

FIG. 5. Vertical shear Reynolds stress ($\overline{u'_{ch}w'}$) estimated using Dewey and Stringer (2007) 5-beam method and bin-averaged by mean flow (colors): a), b) at AI, and c), d) at RP

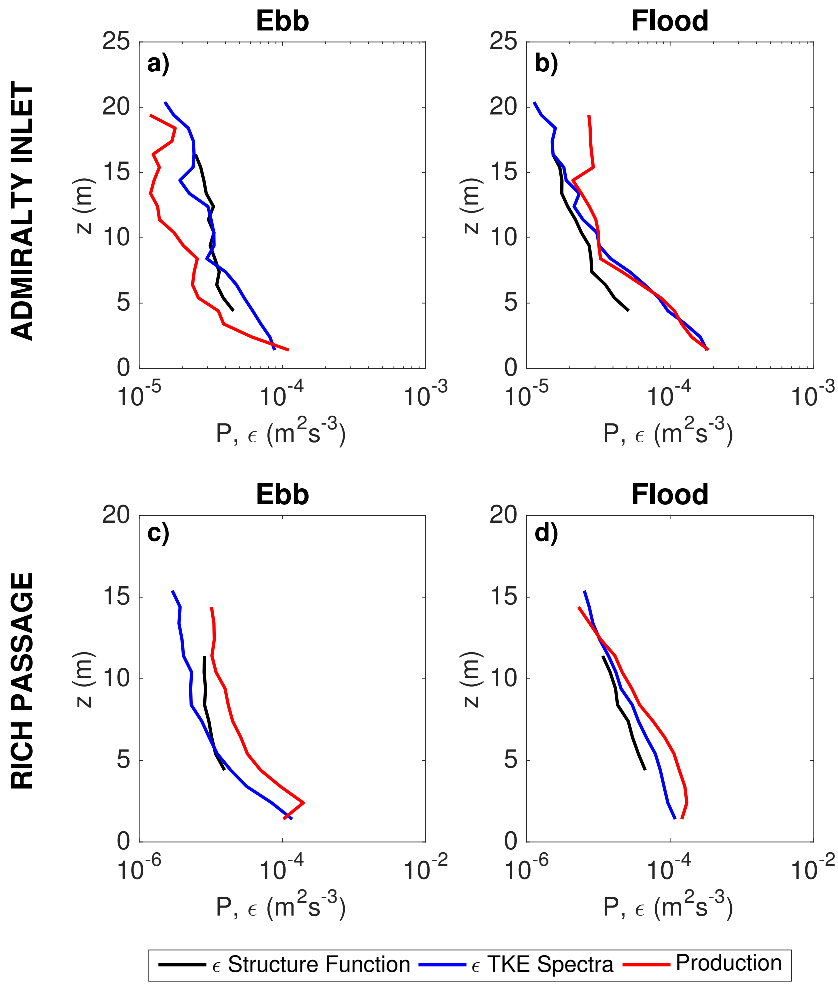

FIG. 6. An approximate TKE budget shown using average TKE dissipation rates from the two methods and TKE shear production from Reynolds stresses: a), b) at AI, and c), d) at RP